Eur. Phys. J. Special Topics **227**, 2361–2374 (2019)

https://doi.org/10.1140/epjst/e2018-800045-4

THE EUROPEAN PHYSICAL JOURNAL SPECIAL TOPICS

Regular Article

Noisy hodgepodge machine and the observed mesoscopic behavior in the non-stirred Belousov–Zhabotinsky reaction*

Optimal noise and hidden noise in the hodgepodge machine

Dalibor Štys[1], Renata Rychtáriková[1,a], Anna Zhyrova[1], Kryštof M. Štys[1], and Petr Jizba[2]

[1] University of South Bohemia in České Budějovice, Faculty of Fisheries and Protection of Waters, South Bohemian Research Center of Aquaculture and Biodiversity of Hydrocenoses, Kompetenzzentrum MechanoBiologie in Regenerativer Medizin, Institute of Complex Systems, Zámek 136, 373 33 Nové Hrady, Czech Republic
[2] Faculty of Nuclear Sciences and Physical Engineering, Czech Technical University in Prague, Prague 1, Czech Republic

Received 10 April 2018 / Received in final form 28 July 2018
Published online 31 January 2019

Abstract. In this paper, we have modified one of the simplest multi-level cellular automata – a hodgepodge machine, so as to represent the best match for the chemical trajectory observed in the Belousov–Zhabotinsky reaction (BZR) in a thin layered planar setting. By introducing a noise term into the model, we were able to transform the central regular structure into the circular target pattern. We further analyze influences of the neighborhood (diffusion process) and internal excitation type of noise. We find that the configurations of ignition points, which give the target patterns, occur only in the interval of the neighborhood excitation noise from 30% to 34% and at the internal excitation noise of 12%. We argue that the BZR occurs on a semi-regular grid – a chemical analogy to a Bénard cell in the viscous fluid, and we discuss the size of the relevant elementary cell. In this way, the BZR is a quintessential example of mesoscopic process, in particular, it does follow neither the deterministic rules of the microscopic system nor the tenet of Boltzmannian statistic physics that only the most frequent events are observed.

1 Introduction

Properties of multi-level cellular automata [1,2] have been examined so far only sporadically. What is known, however, is that their state trajectory critically depends on the number of available levels [3] and that they can be divided into a few-level

* Supplementary material in the form of one zip file available from the Journal web page at https://doi.org/10.1140/epjst/e2018-800045-4

[a] e-mail: rrychtarikova@frov.jcu.cz

automata and true multilevel automata [4]. The border between a few and true multilevel automata was examined only for the so-called square Moore neighborhood and was found to be around 24 levels [3]. Such automata have apparently a sufficient number of levels which allows the system to behave only according to the internal evolution rule (e.g., ratio of constants) independently of the number of levels itself [4].

The *hodgepodge machine* [5] is a type of multi-level cellular automaton which mimics well the final phase of the Belousov–Zhabotinsky reaction (BZR). The *hodgepodge machine* is the simplest of the models which intends to mimic qualitatively the features observed when the BZR is performed in a thin layer. In the context of this paper it is important to mention the simulation of Garcia-Ojarvo and Schimansky-Geier [6] who used the FitzHugh-Nagumo model [7,8] for description of the rise and decay of the excitation. The simulation was performed on a square lattice and may be thus directly compared to the hodgepodge machine. When an adequate level of the Gaussian noise was added, the coexistence of spirals and waves, similar to that in the hodgepodge machine, was observed. The FitzHugh-Nagumo model was originally developed for description of the electrical pulse in the neural system but may be also interpreted in terms of a chemical simplified reaction-diffusion system of chemical transformations.

In our simulations, we modified the model so that it was possible to start from a few ignition points – situation observed in realistic experiments [4]. This enabled us to examine influences of the ignition points as well as the early phases of the trajectory. Eventually, we achieved such a behavior of the hodgepodge machine which is qualitatively compatible with the BZR and consists from an early phase of large center structures – octagons filled by complicated cross-like structures – and ends with a mixture of spirals and waves [4]. The latter suggests that it could be some conceptual overlap between our model and the discrete dynamic networks paradigm proposed in [9].

Our aim here is to promote the idea that the BZR as a typical demonstration of mesoscopic dynamics, i.e., it is neither microscopic, i.e. fully deterministic, nor macroscopic, i.e. represented only by the most probable microstate. The paper is structured as follows: In Section 2, we examine influences of noise on the outputs from the noise-enriched hodgepodge machine (NHM) and discuss the relevance it bears on the BZR. In Section 3, we present results of our simulations and show that the conventional, i.e., "noise-free" hodgepodge machine is in fact a hidden-noise cellular automaton. We also show that many details of the NHM find their direct analogues in the BZR. We further explain the lag phase in the beginning of the BZR using a chemical mechanism analogous to the formation of a regular grid by a Bénard–Rayleigh convection process [10]. Various remarks and generalizations are addressed in Section 4.

2 Materials and methods

2.1 Performance of the chemical reaction

The experiments were performed using the BZR recipe [11]. The reaction mixture included 0.34-M sodium bromate, 0.2-M sulphuric acid, 0.057-M sodium bromide (all from Penta), 0.11-M malonic acid (Sigma-Aldrich) as substrates and a redox indicator and 0.12-M 1,10-phenanthroline ferrous complex (Penta) as a catalyst. All reagents were mixed by hand directly in a 200-mm Petri dish in the sequence mentioned above for 1 min. A special thermostat, which was constructed from a Plexiglas aquarium and a low-temperature circulating water bath-chiller, fixed a reaction temperature at 26 °C.

The chemical waves were recorded by a Nikon D90 camera in the regime of Time lapse (10 s/snapshot) with exposure compensation +2/3 EV, ISO 320, aperture $f/18$, and shutter speed 1/10 s. The original 12-bit NEF raw image format was losslessly transformed to the 12-bit PNG format. The complete courses of the experiment are provided in Videos S1 and S2.

The experiment on a re-started BZR was performed by a manual re-shaking of the reaction vessel after reaching the state of dense waves. The photos of course of the experiment were taken in the time interval of 2 s and consists of 9 cycles of the lengths of 48, 25, 44, 24, 25, 18, 11, 15, and 32 images, respectively.

2.2 Noisy hodgepodge machine model

The NHM of the BZR is essentially the same as in [4] but with the addition of a noise term. We adjusted Wilensky's NetLogo model [12]: The model was run on a square 1-Mpx grid. Ignition centers in $state(t=0) \in [0, maxstate]$ were randomly set on the grid as

$$state(t=0) \;=\; \text{random-exponential}[meanPosition(maxstate+1)]\,, \tag{1}$$

where $maxstate$ is the maximally achievable number of levels of the cell state. Multiplication of each cell state by the $meanPosition$ of the exponential distribution ensured that the simulation started with a small number of the ignition points. Each time step t proceeded in four possible ways:

– When a cell was at the $state(t)=0$, so-called *quiescent*, it was "infected" by surrounding cells according to the equation

$$state(t+1) \;=\; (1+PTN)\left[\text{prec}\left(\frac{a}{k_1}\right)+\text{prec}\left(\frac{b}{k_2}\right)\right], \tag{2}$$

where a and b is a number of cells at the $state \in (0, maxstate)$ and $state = maxstate$, respectively, k_1 and k_2 are characteristic constants of the process.

– When a cell was at the $state(t) \in (0, maxstate)$, its new state was calculated as

$$state(t+1) = \;\text{prec}\left[\frac{state(t)+\sum_{n=1}^{8} state_n(t)}{a+b+1}(1+IEN)+g(1+EEN)\right], \tag{3}$$

where $state_n(t)$ is a state of the nth cell in the Moore neighborhood, which directly surrounds the examined cell, and $g=28$ is another arbitrary constant.

– When a cell was at the $state(t) > maxstate$, then

$$state(t+1) \;=\; maxstate\,. \tag{4}$$

– When a cell achieved the $state(t) = maxstate$, then

$$state(t+1) \;=\; 0\,. \tag{5}$$

In equations (1) and (2), the numerical precision (prec) of 10 decimal points allowed us to realize up to 9×10^{12} states. The individual white noises in equations (1) and (2) were named

– the phase transition noise (PTN): it affects the transition from the state 0 to the first non-zero state,

– the internal excitation noise (IEN): it affects the change of the state due to processes inside the cell, i.e., it influences the constant g [4], and

– the neighborhood (external) excitation noise (EEN): it affects processes related to the values of neighboring cells.

The influences of these kinds of noise were tested by systematic changes of their values. Examples of qualitatively different cases are described in some detail in the following section and shown in Videos S3–S8. The full model is provided in Material S1.

3 Results

3.1 Modeling the Belousov–Zhabotinsky reaction in excitable media and the constructive role of noise

The BZR behavior is not easily comprehensible in terms of the standard Law of Mass Action (which represents the "canonical method" for interpretation of the chemical reactivity) due to the fact that the reaction space is separated into regularly evolving/traveling structures and, thus, one has to consider a large number of interlocked chemical processes. In this work, we report a new stochastic model of the BZR based on the cellular automaton. The model retains some of the key features of the multi-level hodgepodge machine but outperforms this hodgepodge machine in the ability to faithfully mimic the onset stage of the BZR and in the potential to correctly describe the morphology of the evolving wave-spiral patterns.

Figure 1a compares a late (ergodic) stage of the BZR (full data are accessible via S1 Video) at our least spatially constrained (a 200-mm Petri dish) and roil (gentle mixing at 1400 rpm using an orbital mixer) conditions with one of our Wilensky-like model. The structures of the model, which are astonishingly similar to the experiment, arise only at the particular ratio of the model constants independently of the height of the noise. (The most regular spirals and waves, best comparable to the model, are expected to arise in a very gently pre-mixed, homogenous solution of a thin layer in a vessel of the unlimited size which does not spatially constrain evolving waves.) In order to achieve this morphological similarity between the BZR and our simulation, we implemented the following changes into the Wilensky model:

– the enlargement of the cellular grid to 1000×1000,

– start from a very few points which enabled to analyze the behavior of individual centers of emanation,

– a sequence of switching the values of cell states from natural to decimal numbers which extended the span of each cellular state,

– the addition of a uniform white noise to each automaton step which compensated for our limited knowledge of precise underlying mechanism, and

– the extension of the number of achievable states $maxstate$ and rate of the internal cell excitation g up to 2000 and 280, respectively, to smooth the model waves.

The first modification – usage of the larger grid – suppressed to some extent the influence of the non-idealities of the periodic boundaries on the evolution of the model system.

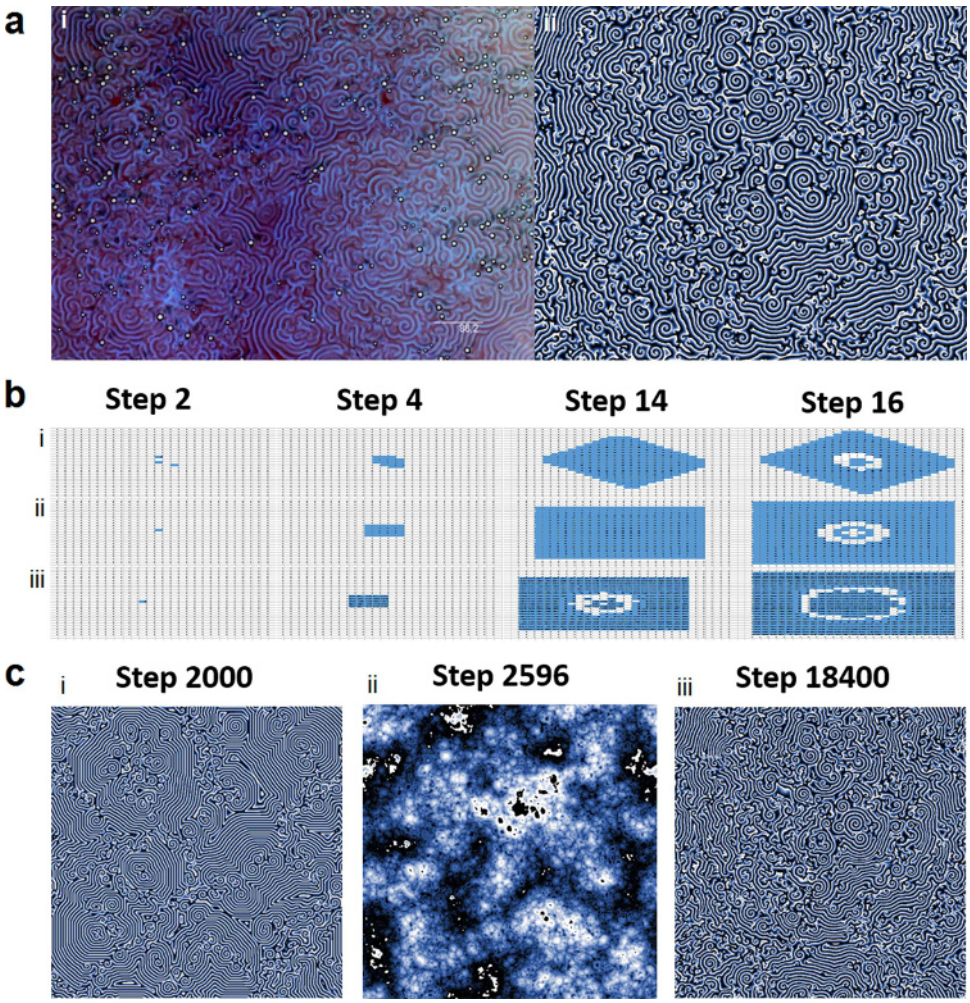

Fig. 1. Illustration of the key aspects of the B–Z model. (a) Comparison of the BZR (i) with the simulation with the levels of noise 9%, 14% and 30% for process 1, 2a, and 2b, respectively, and $k_1 = 3$ and $k_2 = 3$ (ii). Images were expanded so as to have comparable widths of traveling waves. (b) Starting points of the simulations (steps 2, 4, 14, 16). The noise-free simulation with natural number states, $k_1 = 3$ and $k_2 = 3$ in step 2000 (i), the noise-free simulation with natural number states, $k_1 = 2$ and $k_2 = 2$ in step 2596 (ii) and the process described under a in step 18 400 (iii). (c) Final states (limit sets) of processes defined in b. For all processes, $g = 28$ and $maxstate = 200$. In the simulation, the black and white corresponds to 0 and $maxstate$, respectively. Original datasets are supplied in S1 File. The unquestionably inspection of the data has to be done using the original data matrices as demonstrated in Figure 1.

The second intervention into the Wilensky model was performed through a random-exponential function for generation of the starting (ignition) points. This modification, which was originally implemented to start the process from these few centers (ignition points), quite surprisingly increased the morphological similarity between the BZRs and the simulation. The results are depicted in Figures 1b and 1c. In Figure 1b, we present early simulation steps 2, 4, 14, and 16 in process 1 after the ignition. For $k_1 = 3$ and $k_2 = 3$, at least two non-zero points in a proper configuration

a, b were required for the evolution of the waves in the simulation, since at least one addend in process 1 has to be equal to 1. In this case, the early evolution yielded octagons (Fig. 1b, i), while the final state was populated by spirals (Fig. 1c, i). In contrast, if $k_1 = 2$ and $k_2 = 2$, then, e.g. $state(t+1) = \text{round}(\frac{1}{2}) + \text{round}(\frac{0}{2}) = 1$ and the non-zero cell was surrounded by evolving wave of 8 cells in $state(t+1) = 1$. This early evolution resulted in squares with central circular objects (Fig. 1b, ii) which further led to the filamentous structures (Fig. 1c, ii).

The next step softened the definition of the state by allowing 1 decimal place in equations (1) and (2). This modification, however, neglected the condition of the asymmetry for the ignition process and, as a consequence, the development of trajectories could start from any non-zero. Thus, as such, this modification leads only to fuzzy distribution of points. Indeed, increase of the number of decimal places did not have any further effect.

In other words, the implementation of white noise compensated for the need of multiple neighboring points for the realization of the waves' ignition. The different options for setting the ignition points occur randomly and are thus the noise themselves. By the term noise we understand a process with its own internal mechanism which occurs at a rate faster than the rate of the main process (i.e., waves' formation) which it affects. Thus, the original hodgepodge machine was an unrecognized noisy cellular automaton.

The only effect of higher number of decimal points were smoother edges in the spiral shape.

The detailed comparison of the models and experiment is given in Figure 2a. The sequence of simulated structures is the following:

- The simulation grid is filled with systems of square dense waves. This has not been observed in the experiment and we interpret it as a *lag phase*, which precedes the observed formation of circular waves.
- Circular structures emanate from the center of square waves.
- At the certain state, the simulation grid is nearly covered by large circular structures. A few spirals occur at places where the regular wavefront was distorted and break into a first generation of spirals.
- The final state is similar to that in the simulation where the states are natural numbers, $k_1 = 3$, and $k_2 = 3$, however, the waves are about 2 grid elements thicker.

Let us mention further key similarities between our simulation and actual experiments (Figs. 2b and 2c):

- The chemical waves do not interfere like material waves but merge.
- The chemical waves do not maintain the shape (as, e.g., solitons [13]).
- The morphology of interacting patterns (merger of patterns) in simulations has comparable traits as in real experiments.
- Quantitative features of the limit sets, i.e., the last evolutionary stage of the wave-spiral patterns can be set as close as possible to actual experimental data by an appropriate choice of the parameter range.

3.2 Influence of the noise

In Figure 3, we show a sketch of the research on the increase of neighborhood and internal kinds of excitation noise. Most cases gave a typical trajectory as shown in

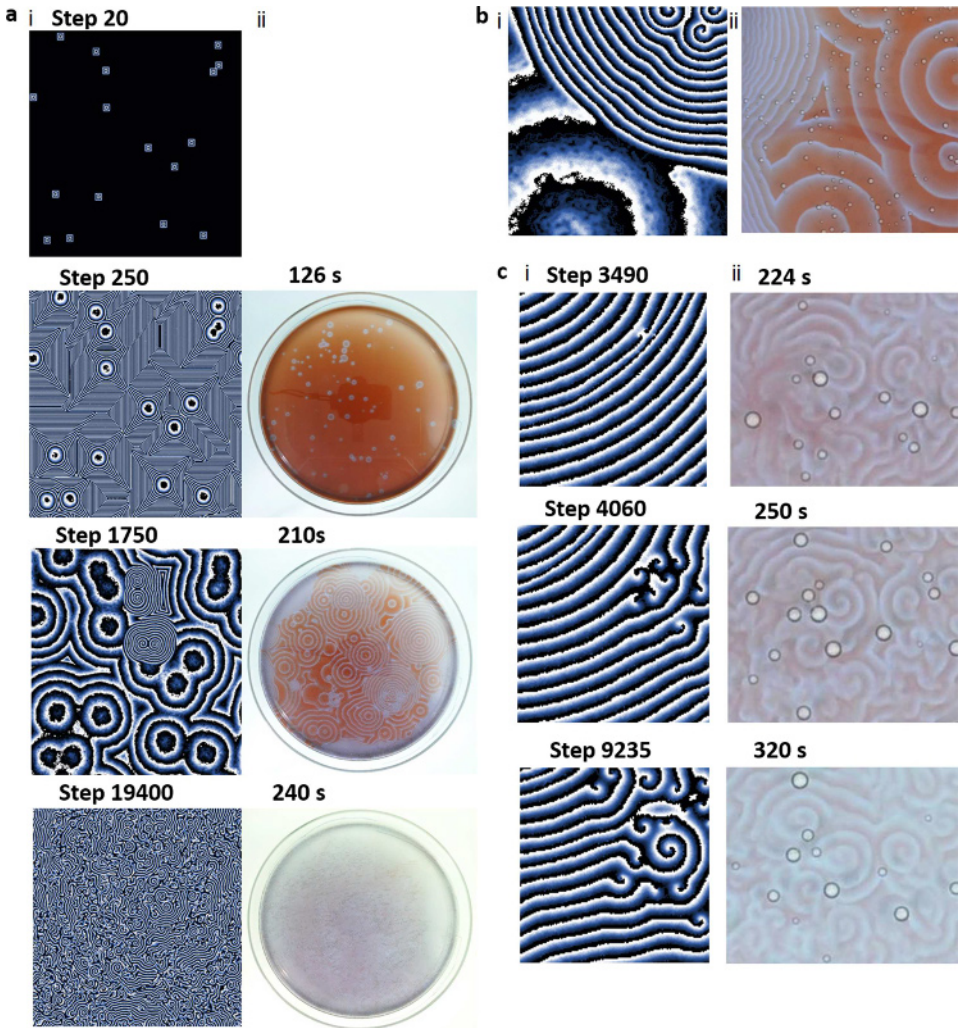

Fig. 2. Similarities between the trajectories of the simulation and of the BZR. (a) Selected states of the simulation (i) and corresponding images from the course of the experiment (ii). The early stage of the experiment corresponds to the lag phase of the experiment when no waves evolve. For the later stages of the simulation, corresponding structures were found in the experiment. (b) Sections of images which show wave merging. Similar behavior has not been found for material waves and another wavelike structures and indicates that threshold-range cellular automata (i) are proper models for phenomena observed in the BZR (ii). (c) States in formation of spirals. In the simulation (i), the distortion of the dense waves leads to their merging which is the source of formation of spirals. In the experiment (ii), the source of the distortion is often a bubble of carbon dioxide. Otherwise, the formation of spirals is similar to the experiment. For all processes, $g = 28$, $maxstate = 200$, $k_1 = 3$ and $k_2 = 3$. In the simulation, the black and white corresponds to 0 and $maxstate$, respectively.

Figure 1. Images in Figure 3 show sections of the 1600th step of the simulation, where the spiral-based structures prevail over the central circular target pattern. We observed some remnants of the circular structures followed by spirals and waves evolving around them. However, both central circular structures and systems of spirals and waves slightly differ. The exception occurred at neighborhood and internal excitation

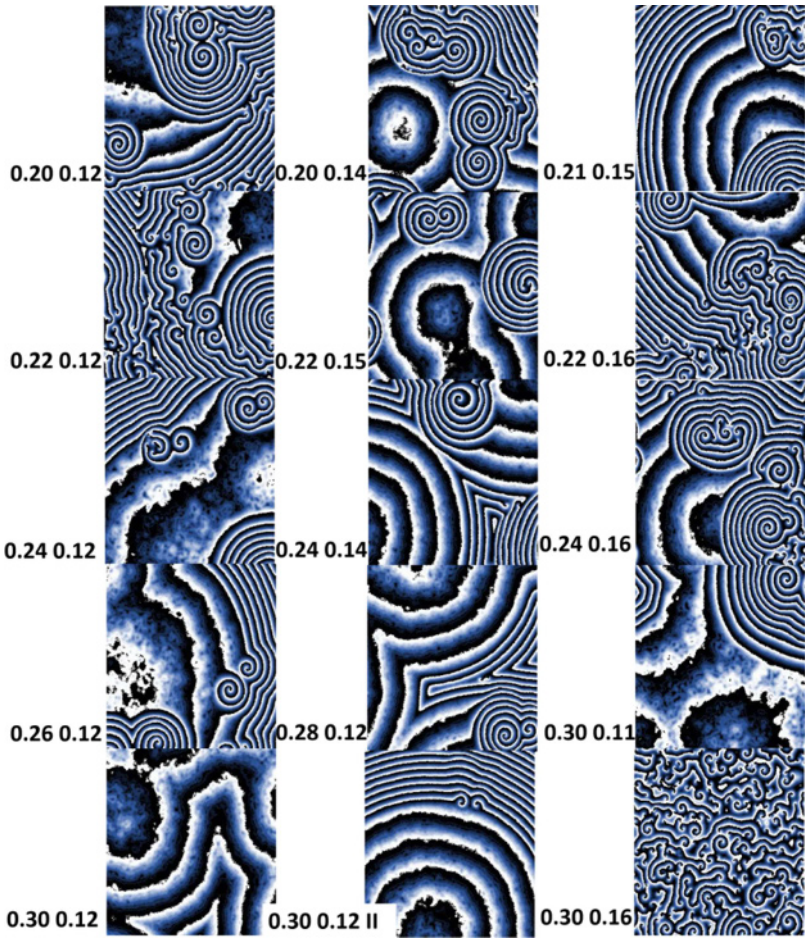

Fig. 3. Sections of steps 1600 of the simulations at different levels of external (the first number) and internal (the second number) excitation noise. The Roman numeral II (*bottom middle*) denotes the second experiment. Only at the internal and external (neighborhood) excitation noise of 30% and 12% (*bottom left*), respectively, mutual geometries of initial ignition points for which no spirals were formed were found. At any higher density of ignition points and different geometries, spirals were formed even at these combinations of noises.

noise of 30% and 12%, respectively (*bottom left* and *bottom middle*), where, in some cases, we did not observe any spirals. In contrast, the combination of neighborhood and internal excitation noise of 30% and 16% (*bottom right*) resulted in the fast evolution of spirals and waves which prevented the formation of circular waves.

3.3 Re-shaking experiment

Figure 4 shows the course of the experiment on the re-started BZR. The process (*cycle 1*) started by the evolution of circular waves. Each sub-experiment was stopped after reaching a phase of dense waves and the reaction vessel was re-shaken. This process was repeated 9 times. Upon re-shaking, the waves gradually lost regularity and became thicker, the diameters of target patterns increased (*cycle 3*) and the waves evolved mainly at the vessel's border (*cycle 4*). Similar phenomena were observed in a

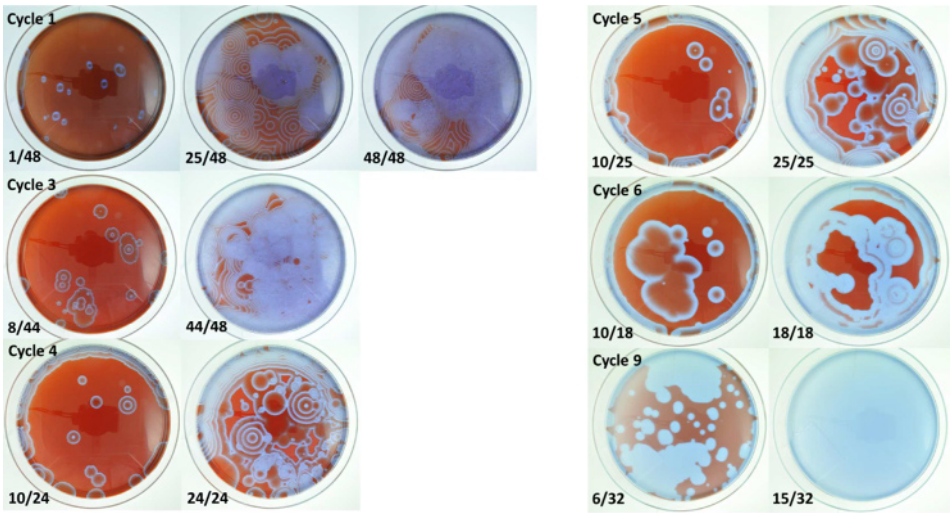

Fig. 4. Re-start of the B-Z reaction (9 cycles). The number ratio X/Y means the Xth image from a Y-image series.

Petri dish of a smaller diameter. Further thickening of waves (*cycle 5*) led eventually to merging of circular waves (*cycle 6*) up to a complete filling of circular waves' centres (*cycle 9*). The next mixing did not lead to re-formation of the red-colored state.

In the early phase and, namely, upon gentle mixing (as shown in Fig. 1) the circular waves are highly regular. At later stages, upon re-shaking, the wavefronts became undulated and more similar to those observed in the NHM simulation. Finally, the waves thickened to the extent that the formation of structures was no more possible.

This experiment demonstrates that the depletion of reactants does not change the shape of observed waves and their course (order) but causes thickening of the traveling waves and shortens time to reaching the ergodic state. The ergodic state, both in the experiment and in the model, is characterized by a coexistence of spirals and waves.

3.4 Mesoscopicity and the size of the elementary spatial unit

When noise matters, an observed process is typically mesoscopic. It does follow neither the deterministic rules of the microscopic (or purely mechanical) system nor the statistical-physics tenet of Boltzmannian statistic physics that only the most frequent events are observed. The success of the simulation described in this article is based on the existence of the minimal spatial element to which all processes are referred. Indeed the simplest explanation is that the space is segregated into elementary units similar to those observed in viscous fluids at temperature gradients, i.e., to the Bénard cells [10]. With this hypothesis, we have examined the size of the elementary unit.

Figure 5 shows the analysis of wave profiles in the hodgepodge model. Figure 5a shows the influence of the $g/maxstate$ ratio on the final phase of the model in the noise-free and discrete system when no decimal numbers are allowed. The $g/maxstate$ ratio corresponds to the number of timesteps of the simulation at which the maximal excitation was achieved. The timestep may be also understood as a measure of the ratio between a "diffusive" process (the first term in Eq. (3)) and a zero-order chemical reaction (the second term in Eq. (3)) when the first term is always realized in one timestep. A low $g/maxstate$ ratio, i.e., a fast reaction process in comparison to the

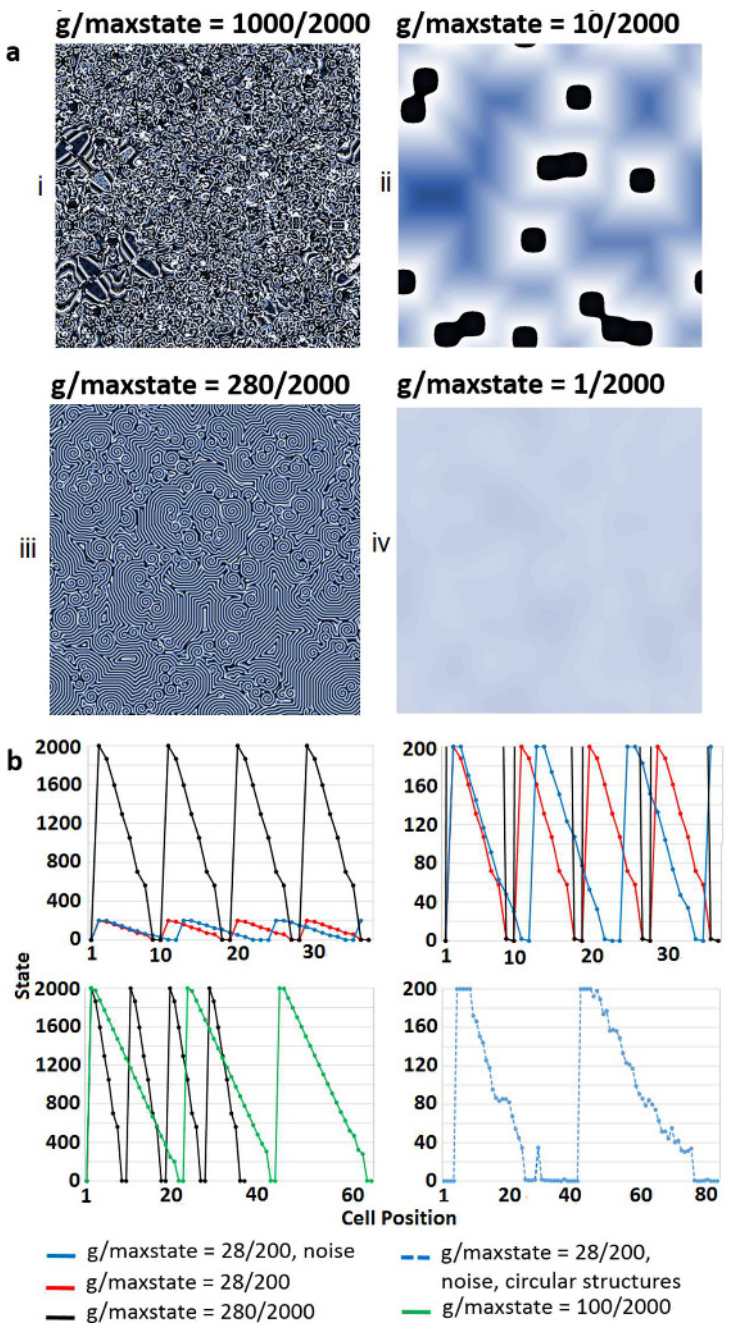

Fig. 5. Ratio of processes 2a and 2b determines the size of elementary unit and the type of state trajectory. (a) Images of later states of simulation at different $g/maxstate$ ratios, $k_1 = 3$, $k_2 = 3$ and $noise = 0$. At $g/maxstate = 1000/2000$ (i), spirals evolve into forms of ram's horns. To the opposite, $g/maxstate = 10/2000$ (ii) does not form spirals. At $g/maxstate = 1/2000$ (iv), the process is fully diffusive. At $g/maxstate = 280/2000$ (iii), the trajectory is almost identical to the experimental trajectory. (b) The intensity profiles of waves at different $g/maxstate$ ratios. Decrease of the $g/maxstate$ ratio leads to the broadening of waves. The intensity profile of the circular structure is very noisy. In the simulation, the black and white corresponds to 0 and $maxstate$, respectively.

diffusive one, leads to narrow waves and short spirals (e.g., Fig. 5a-iii). At a very low $g/maxstate$ ratio, waves do not fully develop and spirals do not arise (e.g., Fig. 5a-iv).

Figure 5b depicts several profiles of waves taken in the direction orthogonal to the wave development. As shown, the formation of wave in the system with and without the introduced noise, respectively, takes different times. In the noise-free processes (e.g., at the $g/maxstate$ of 28/200 and 280/2000, *upper*), the wave is fully formed in 10 steps, while, in the simulation when noise is induced (see $g/maxstate = 28/200$), the formation of the wave takes 13 steps. At $g/maxstate = 100/2000$ (*lower left*), the waves are as broad so that they do not fully separate. For comparison, Figure 5b includes the profile of the early circular wave (*lower right*).

The striking similarity of the simulation to real experiment intensity profiles of dense waves (Figs. 1, 5 and 6) motivated us to guess the number of molecules per an elementary spatial unit (i.e., the pixel of experimental wave). The number of elementary units per the width of the wave was in the range of 10–20. Since the average width of the wave was 1.5 mm, the elementary unit had 0.07–0.15 mm. The solution above the elementary unit had thickness and volume of 0.5 mm and 10^{-2} mm^3, respectively. Then, the solution contained ca. $3{\times}10^{13}$ and 10^{10} molecules of water and reactants per elementary unit, respectively. This number lies within the thermodynamic limit. The source of the mesoscopicity has to be sought in the physico–chemical dynamics. It means that only a few energetic/re-organizational events occur within a given time. Since an elementary spatial unit contains roughly 10^{10} molecules of reactants, it is likely that we are dealing with a phase separation which gives rise to structures of an analogous type as, e.g., in liquid crystals [13].

4 Conclusions

In the BZR, the target circular waves are always overcome by dense waves and spirals. Dense waves are typically evolving at the border of a Petri dish due to the non-idealities of the spatial geometry, while spirals evolve from the origin located at the center from micro-bubbles (again from a spatial inhomogeneities).

The re-shaken experiment excludes any simple chemical interpretation of the decay of observed structures. It is not the depletion of chemicals which leads to the transformation of circular waves – target patterns – to dense waves and, finally, to the mixture of spirals and dense waves. In the wide range of concentrations, when the thickness of waves is not broader than the diameter of the Petri dish, the general behavior of the BZR is qualitatively identical. The self-organization in the BZR is a process which is separated from a concrete chemical reaction. This fact justifies the search for a model of self-organization which would describe the reaction and ignore the actual chemical process.

In the numerical simulations presented in this article, it has been found that, at certain configurations of ignition points, there is a lower and upper limit of the noise at which the whole simulation grid is filled with circular structures – target patterns – and the spirals-waves phase never occurs. This happens when combination of neighborhood (external) excitation noise (EEN) is from 30% to 34% with the internal excitation noise (IEN) of 12%. The spatial inhomogeneity which lead to the evolution of spirals and waves at unfavorable conditions is not properly described by this model. However, at certain combinations of the geometry of ignition points, spirals are formed even in this case.

The spirals are formed also in the original hodgepodge machine. This can be observed in cases when the ignition constants k_1 and k_2 are bigger than 2. Our interpretation of this fact is that the multitude of possible realizations of the ignition points serves as a kind of noise. Thus, for the formation of spirals and waves, the noise is a necessary condition. This noise is in fact the phase transition noise (PTN)

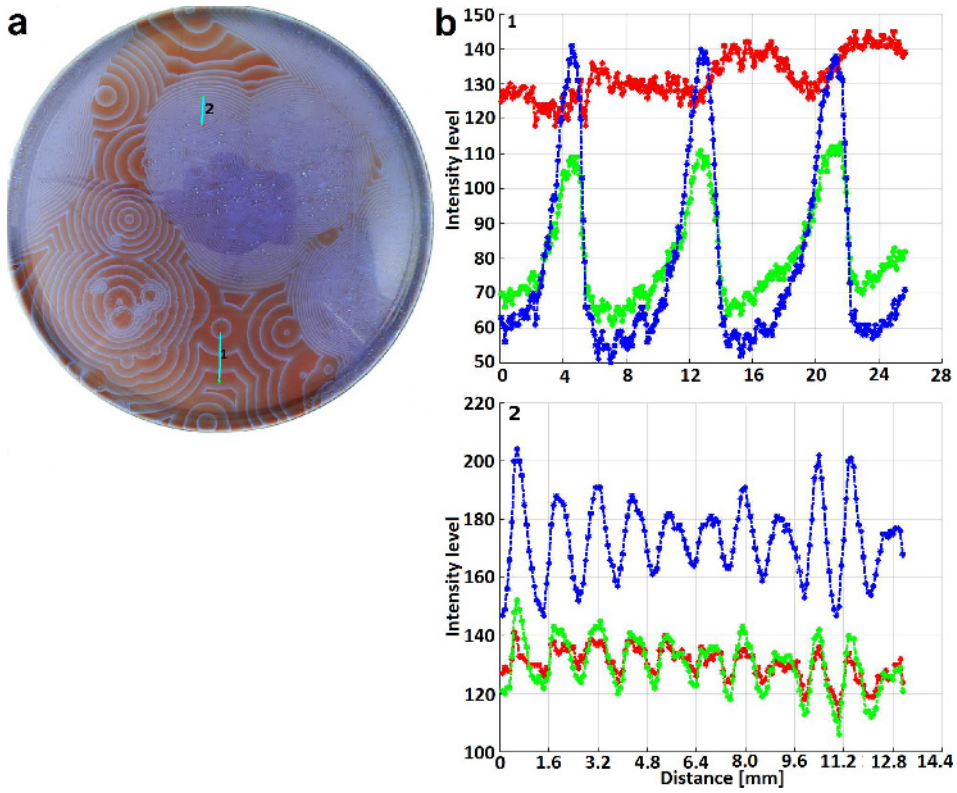

Fig. 6. Analysis of traveling waves in the Belousov–Zhabotinsky experiment. (a) Figure with identified wave profiles. (b) Intensity profile of the early circular wave (1) and later dense wave (2). Three colors represent camera channels.

but of a very specific spatial distribution. In our numerical simulations this PTN was mimicked by a combination of the proper IEN and EEN.

Differences in structures and dynamics shown in the re-shaking experiment (Fig. 4) – the undulation of circular waves, thickening, doubling of wavefront, etc. – indicate that there exist numerous individual processes which play a rôle in the formation of the patterns in the BZR. All these processes have rates comparable to the bottleneck process which determines the characteristic reaction time. Unfortunately, at present it does not exist experimental procedure for identification of these processes. We know a lot of chemicals but we do not know which breakage of individual chemical bond or diffusion constant corresponds to the bottleneck process. As described in [4], this is analogous to the thickening of the wave observed in the "noise-free" hodgepodge machine due to the decrease of the $g/maxstate$ ratio. Thus, the model has a potential to explain this aspect of the experiment as well.

We conclude that the noisy hodgepodge machine – NHM – is one of the simplest (if not the simplest) approximations to all natural processes occurring in a plane and leading to formation of coexistence of spirals and waves as well as to diffusive structures. It provides all basic stages observed in the experiment and indicates (and restricts) possible geometrical and kinetic rules. The ratio of two slowest processes close to 7:2 and the $g/maxstate$ value 1:7 lead to the best approximation of observed reality [4]. In the experiment, we observe the dominant "hodgepodge" process combined with a number of individual processes. The competing processes, occurring at

a slower but comparable rate, have the character of noise which may be even spatially non-isotropic. They are only roughly simulated by the white noise used in the NHM. Using the different kinds of noise, the circular waves are stabilized and several frequencies are observed.

In any case, the dynamical co-existence of spirals and dense waves is the ergodic state in all observed cases. It is clear that the ergodic state is not a state of chemical equilibrium. Even the homogenously blue color observed at the end of the re-shaking experiment is not the chemical equilibrium state. It is still a dynamic state where the blue waves cannot be observed. The true chemical equilibrium occurs only when all Fe^{2+} ions are oxidized and precipitated in the form of iron(III) oxide.

In summary, this article supports the hypothesis that the BZR consists of an initial (lag) phase in which a regular grid of spatial cells is formed. Within this grid, the process of chemical "communication" occurs due to diffusion between these cells. Inside each of the cell develops a process whose chemical character may be, perhaps, described by one of the schemes developed for oscillating process in the mixed vessel.

The earlier observation of Garcia-Ojarvo and Schimansky-Geier [6] who showed that noise induces the formation of spirals in the FitzHugh-Nagumo model on a regular grid was at least qualitatively identical to our observation of spirals and waves at the late ergodic stage of the BZR. Possibly, the same mechanism of generation of spirals and waves may be applied to the whole class of similar real excitable media operating in "two-dimensional" conditions, e.g., in a sufficiently thin layer or in a living cell monolayer. The ergodic pattern in the final phase of the systems of the excitable media can be thus achieved either as a result of "noise" generated due to two or more non-zero cells in the vicinity of the ignition point, or by introduction of two different levels of flat (white) noise into "reaction" and "diffusion" element of the excitable medium, respectively, or by the application of the Gaussian noise to the resulted value. This fact that the same final ergodic state is achieved by three different way demonstrates that the coexistence of spiral and waves is a final state for a wide spectrum of noisy excitable media.

The stringent correspondence of the simulation on a discrete grid to the chemical experiment strongly supports the hypothesis on the formation of a grid of cells analogous to the Bénard cells in viscous liquid [10] or to elementary cells in liquid crystals [13]. This observation opens numerous new questions, namely, to which extent the continuous differential equations are appropriate tools for description of natural processes, at least those which lead to spirals or turbulences.

This work was supported by the Ministry of Education, Youth and Sports of the Czech Republic – projects CENAKVA (No. CZ.1.05/2.1.00/01.0024), CENAKVA II (No. LO1205 under the NPU I program), the CENAKVA Centre Development (No. CZ.1.05/2.1.00/19.0380) – and from the European Regional Development Fund in frame of the project Kompetenzzentrum MechanoBiologie (ATCZ133) in the Interreg V-A Austria – Czech Republic programme and by project GAJU 017/2016/Z. P.J. was supported by the GAČR Grant 17-33812. Authors thank to the anonymous reviewer for the comments which helped them to improve the interpretation of the results presented in the paper.

Author contribution statement

D.Š. designed the noisy hodgepodge machine model, performed the noisy hodgepodge machine simulations, analyzed their results and prepared the first draft of the paper. A.Z. performed and analyzed the chemical experiments on the Belousov-Zhabotinsky reaction. K.-M.Š. performed the hodgepodge machine simulations and classified the simulation results. R.R. developed the algorithms for analysis of experimental datasets, contributed to the theoretical discussions, coordinated manuscript

preparation, and edited its final version. P.J. masterminded the theoretical discussion and editing of the manuscript.

References

1. V.K. Vanag, Physics–Uspekhi **42**, 413 (1999)
2. M. Gerhardt, H. Schuster, J.J. Tyson, Science **30**, 1563 (1990)
3. S. Hiltemann, Multi-coloured cellular automata, Bachelor thesis, Erasmus Universiteit, Rotterdam, The Netherlands, 2008
4. D. Štys, T. Náhlík, A. Zhyrova, R. Rychtáriková, Š. Papáček, P. Císař, in *HPCSE 2015*, Lect. Notes Comp. Sci. **9611**, 171 (2016)
5. A.K. Dewdney, Sci. Am. **225**, 104 (1988)
6. J. García-Ojalvo, L. Schimansky-Geier, Europhys. Lett. **47**, 298 (1999)
7. R. FitzHugh, Bull. Math. Biophys. **17**, 257 (1955)
8. J. Nagumo, S. Arimoto, S. Yoshizawa, Proc. IRE **50**, 2061 (1962)
9. A. Wuensche, *Exploring discrete dynamics* (Luniver Press, 2011)
10. A.V. Getling, *Rayleigh-Bénard convection: structures and dynamics* (World Scientific, 1998)
11. J. Cohen, http://drjackcohen.com/BZ01.html
12. U. Wilensky, NetLogo B-Z Reaction model (Center for Connected Learning and Computer-Based Modeling, Northwestern University, Evanston, IL, 2003), http://ccl.northwestern.edu/netlogo/models/B-ZReaction
13. M. Blasone, P. Jizba, G. Vitiello, *Quantum field theory and its macroscopic manifestations. Boson condensation, ordered patterns and topological defects* (Imperial College Press, Cambridge, UK, 2011)